Calculations of the Optical Spectra of Hydrocarbon Radical Cations Based on Koopmans' Theorem

Stephen F. Nelsen,*,† Michael N. Weaver,† Daisuke Yamazaki,‡ Koichi Komatsu,‡ Rajendra Rathore,# and Thomas Bally*,§

Department of Chemistry, University of Wisconsin, 1101 University Avenue, Madison, Wisconsin 53706-1396, Institute for Chemical Research, Kyoto University, Uji, Kyoto 611-0011, Japan, Department of Chemistry, Marquette University, P.O. Box 1881, Milwaukee, Wisconsin 53201-1881, and Department of Chemistry, University of Fribourg, 1700 Fribourg, Switzerland

Received: September 28, 2006; In Final Form: December 12, 2006

The first few bands in the optical spectra of radical cations can often be interpreted in terms of A-type transitions that involve electron promotions from doubly occupied to the singly occupied molecular orbital (SOMO) and/or B-type transition which involve electron promotion from the SOMO to virtual molecular orbitals. We had previously demonstrated that, by making use of Koopmans' theorem, the energies of A-type transitions can be related to orbital energy differences between lower occupied MOs and the highest occupied MO (HOMO) in the neutral molecule, calculated at the geometry of the radical cation. We now propose that the energies of B-type transitions can be related similarly to energy differences between the lowest unoccupied MO (LUMO) and higher virtual MOs in the dication, also calculated at the geometry of the radical cation, by way of an extension of Koopmans' theorem to virtual MOs similar to that used sometimes to model resonances in electron scattering experiments. The optical spectra of the radical cations of several polyenes and aromatic compounds, the matrix spectra of which are known (or presented here for the first time), and for which CASSCF/CASPT2 calculations are available, are discussed in terms of these Koopmans-based models. Then the spectra of five poly(bicycloalkyl)-protected systems and that of hexabenzocoronene, compounds not amenable to higher level calculations, are examined and it is found that the Koopmans-type calculations allow a satisfactory interpretation of most of the features in these spectra. These simple calculations therefore provide a computationally inexpensive yet effective way to assign optical transitions in radical ions. Limitations of the model are discussed.

Introduction

The groups of Haselbach,[1−4] Zahradnik,[5] and Shida[6,7] established that, when the geometry reorganization upon electron removal is small (as it is for hydrocarbons containing conjugated π-systems), the energy differences between higher energy peaks and the first peak in the photoelectron spectrum of the corresponding neutral compound relate to the energies of those electronic transitions in the radical cation that involve promotion of an electron from the manifold of doubly occupied MOs to the singly occupied MO (SOMO) of the radical cation (A-type transitions according to the nomenclature of Hoijtink[8] and Zahradník,[9] cf. Scheme 1). Haselbach, Shida, and co-workers pointed out the relationship of these observations to Koopmans' theorem,[10] which states that ionization potentials of neutral, closed shell molecules are equal to the negative of their orbital energies, $-\epsilon_i$. However, optical transitions involving electron promotion to virtual orbitals, (B- and C-type transitions in Scheme 1), which bear no direct relation to Koopmans' theorem, are also observed in radical ion spectra.[11−13]

SCHEME 1: Generic MO Scheme for a Radical Cation (Left Side) and a Radical Anion (Right Side)

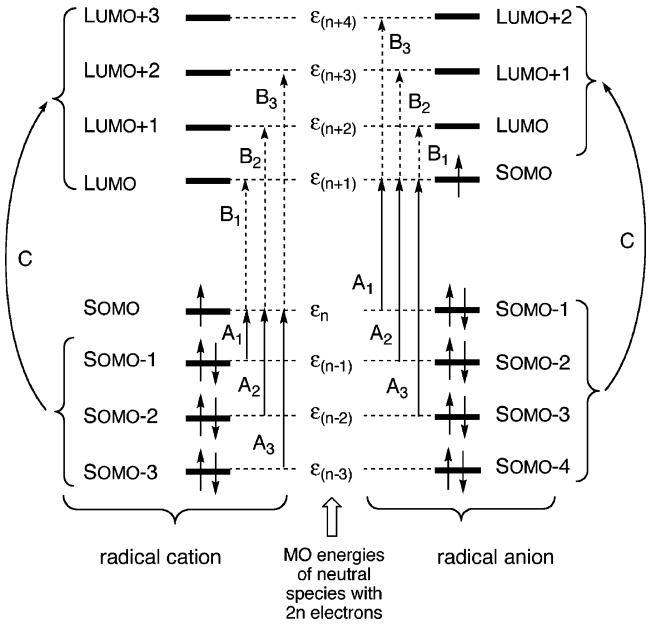

* Corresponding authors. E-mail: S.F.N., nelsen@chem.wisc.edu; T.B., Thomas.Bally@unifr.ch.
† University of Wisconsin.
‡ Kyoto University.
# Marquette University.
§ University of Fribourg.

10.1021/jp066384i CCC: $37.00
Published on Web 02/09/2007

On the basis of the above concepts, we concluded some time ago that the energies E_i of A-type transitions in a radical cation (where the *n*th MO is singly occupied) should correspond to *differences* of orbital energies $\Delta\epsilon_i = \epsilon_n - \epsilon_{(n-i)}$ calculated for the corresponding neutral, closed-shell compound containing 2*n* electrons. Furthermore, we demonstrated that optical transition energies of radical cations can be successfully predicted using this approach based on Koopmans' theorem, even for systems that undergo large geometry changes upon ionization, by carrying out the calculations at the optimized geometries of the radical cations (we termed these "neutral at cation geometry" or NCG calculations). These calculations were also applied to the $\sigma \rightarrow \pi$ transitions in some bis(bicyclic) tetraalkylalkene radical cations.

Our first applications of this method referred to hydrazine and tetraalkylhydrazine radical cations that were constrained to various degrees of bending by structural effects,[14−17] and to the $\sigma \rightarrow \pi$ transitions in some bis(bicyclic) tetraalkylalkene radical cations.[18] In these cases the energy gap between the HOMO and HOMO−1 level in the neutral closed-shell species (i.e., transition A_1 in Scheme 1) was found to be very close to the energy of the lowest observed transition (or to that calculated by more sophisticated methods). At the time, these calculations were carried out using a special version of Clark's semiempirical VAMP program that also permitted calculation oscillator strengths for A-type transitions.[19]

In *radical anions*, the lowest energy transition is usually of B-type; i.e., they involve electron promotion into virtual MOs whose energies, $\epsilon_{(n+j)}$ in Scheme 1, have a priori no physical meaning. Therefore, an extension of the above Koopmans-based approach to radical anions is not straightforward. Koopmans' theorem works quite well in practice, at least for valence MOs, due to a fortuitous cancellation of errors (neglect of orbital relaxation and of the change in correlation energy on ionization).[20] This cancellation does, however, not necessarily carry over to states that involve excitations into virtual MOs. In spite of this, researchers who study resonances (transitory radical anion states) in electron scattering experiments[21] have used the energies of virtual MOs to predict the energies at which these resonances occur, i.e., to apply Koopmans' theorem to calculate electron affinities much like one used it to calculate ionization potentials. It was found that such calculations can, however, only be brought into reasonable agreement with experiment if some scaling is applied to the virtual orbital's energies.[22] We have recently realized that our Koopmans-based approach may work even without scaling because B-type transitions involve energy *differences* between virtual MOs, analogous to A-type transitions of radical cations which relate to energy differences between doubly occupied MOs.[23] Indeed, such calculations gave predictions in good agreement with experiment for a series of dinitro radical anions bridged by aromatic rings[24] and rationalize the spectra of a series of *p*-phenylene-bridged radical cations and anions that have heteroatom charge-bearing units.[25]

The picture that is conveyed by Scheme 1 is of course a rather crude one. First, it does not show that addition or removal of electrons has a large effect on the energies of all orbitals. Second, in a model based on one-electron wavefunctions, the presence of an unpaired electron in the HOMO of a molecule splits the degeneracy of all subjacent orbitals containing α and β electrons because, due to operation of the Pauli principle, the integrated repulsion between electrons of like spin is lower than that between electrons of opposite spin. Thus, modeling radical ions in terms of restricted wavefunctions is not really appropriate.[26] These two effects are illustrated in Figure 1 for the B3LYP-MOs of hexatriene.

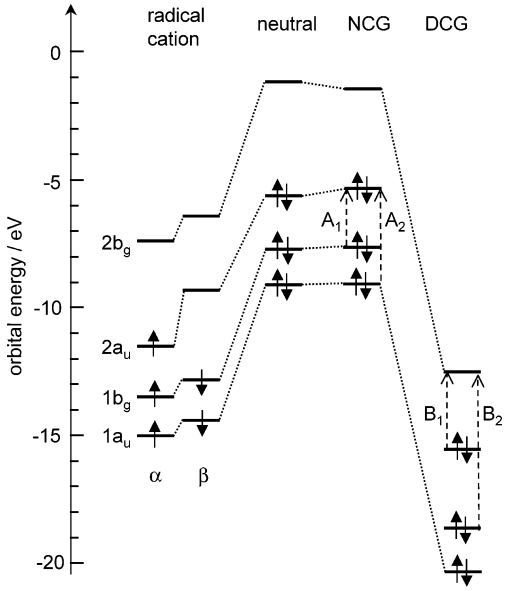

Figure 1. MO energies from (U)B3LYP/6-31G* calculations on the hexatriene radical cation, the neutral compound, at its own equilibrium geometry ("neutral"), and that of the radical cation ("NCG"), as well as the dication at the radical cation geometry ("DCG").

An important caveat concerns the fact that Scheme 1 (and Koopmans' theorem) is based on a one-electron picture of electronic excitation. It has been known for a long time that most excited states of neutral molecules cannot be described correctly by single excited configurations, which is why most semiempirical or ab initio methods designed to predict excitation energies and transition moments account for the mixing of excited configurations of the same symmetry (configuration interaction, CI).

The great success of Koopmans' theorem in the assignment of photoelectron spectra[27] would seem to suggest that (doublet) excited states of radical cations lend themselves better to a one-electron description than do the open-shell singlet excited states of neutrals. Many-electron calculations show that the first few A-type transitions of radical cations are indeed often well described by a single configuration, although notable exceptions are known (e.g., the polyene radical cations that will be described in the next section). In contrast, B-type excitations often mix with higher A-type excitations (or with those of C-type with which we will not deal explicitly in this work). We will therefore have to keep an eye on this possible limitation of Koopmans-based calculations of radical ionic excited states, especially when dealing with higher excited states.

In this paper we test Koopmans-based calculations on hydrocarbon radical cations by comparing observed spectra with calculated ones (A-type transitions from NCG, B-type transitions from DCG calculations) and/or with calculations obtained at the CASSCF/CASPT2 level, which has proven to be very reliable in assigning or predicting the spectra of numerous organic radical cations.[28−35] This comparison will allow us to stake off the scope and limitations of the Koopmans-based method in assigning radical ion spectra.

Although the original formulation of Koopmans' theorem[10] is in terms of Hartree−Fock theory, we found that the energies of Kohn−Sham orbitals from density functional calculations are better suited than those of HF orbitals for the present type of calculations. We make use of the popular B3LYP combination of exchange and correlation functionals and employ the

standard 6-31G* basis set (adding more basis functions was found to improve the results only marginally).

When discussing optical spectra of radical ions within a single-electron approximation, it is convenient to label the orbitals relative to the SOMO, which is the target or the origin of A- and B-type electron promotions, respectively. Therefore, the labels A_i and B_i, which are used in the literature to designate such excitations,[9] will also be used to identify the MOs that are the origin in A_i transitions (SOMO$-i \rightarrow$ SOMO) as A_i, and those which are the target MOs in the B_j transitions (SOMO $\rightarrow$ SOMO$+j$) as B_j.

We calculate the oscillator strength f for Koopmans-based calculations using Weinhold's natural bond orbital (NBO) program[36] to obtain the transition dipole moment matrix in the molecular orbital basis for the transitions. These calculations are accomplished using the "DIMO" keyword in the \$NBO keylist of a Gaussian 98 or 03 computation (which requires that NBO 5.0 or higher be used). The oscillator strengths may then be calculated using eqs 1 and 2.

$$\mu_{12} = 2.5418 \times \sqrt{\mu_x^2 + \mu_y^2 + \mu_z^2} \qquad (1)$$

$$f = E \times 1.085 \times 10^{-5} \times \left(\frac{\mu_{12}}{4.8032}\right)^2 \qquad (2)$$

1. Polyene Radical Cations. We will begin the comparison with the radical cations of the polyenes butadiene (**1**), hexatriene (**2**), and octatetraene (**3**), whose optical spectra were recorded some time ago,[13] and for which complete CASSCF/CASPT2 calculations have been carried out.[37] Table 1 juxtaposes these results to those of the present Koopmans-based calculations.

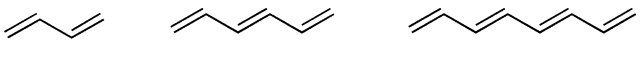

1 **2** **3**

The essential features of the electronic structure of polyene radical cations can be explained on the basis of Scheme 2:[38] The first two allowed transitions involve the A_1 (SOMO$-1 \rightarrow$ SOMO) and B_1 (SOMO $\rightarrow$ LUMO) excitations. With increasing chain length these two excited configurations, which are always of the same symmetry within the C_{2h} point group, move closer in energy, and hence their mixing becomes more pronounced. As the Koopmans-based predictions in the right-most column of Table 1 "measure" the energies of pure configurations, i.e., $E(A_1)$ and $E(B_1)$ in Scheme 2, it is not surprising that they invariably predict the energy of the first transition (E_1) too high and that of the second one (E_2) too low. Obviously, polyene radical cations constitute a class of molecules where the Koopmans-based approach fails to correctly predict the energies of the first few transition or their intensities well, due to the importance of CI, even for the first two excited states. Nevertheless, they produce qualitatively the same assignment of the observed bands, and they may give an indication of how large the energy shifts caused by CI are.

SCHEME 2: Electronic Structure of Polyene Radical Cations

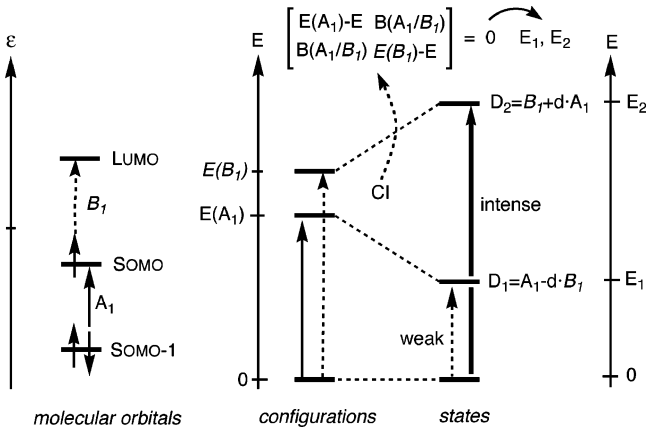

2. Naphthalene and Anthracene Radical Cation. Another class of radical cations for which well-resolved optical spectra extending well into the UV are available are those of the condensed aromatic hydrocarbons, naphthalene **4**[31] and anthracene **5**[20] (as well as some derivatives of naphthalene[31] that we will not discuss in detail here). For $\mathbf{4}^{\bullet+}$ CASSCF/CASPT2 calculations have been published,[31] those for $\mathbf{5}^{\bullet+}$ are presented here for the first time. The spectra obtained in argon matrixes are juxtaposed to schematic representations of the computational results in Figures 2 and 3, and Table 2, in which the orbitals involved in the different transitions are shown, lists the results numerically.

For both aromatic radical cations, the first electronic transition is electric dipole forbidden and will not be considered here. In both cases the first allowed transition corresponds predominantly to A_2 excitation, and it is therefore predicted quite well by the Koopmans-based method. The second allowed transition has a very weak oscillator strength in both radical cations, but its nature is different: in $\mathbf{4}^{\bullet+}$ it corresponds to A_3 excitation which is, however, mixed significantly with the B_1 excitation according to the CASSCF calculations. Hence it is not surprising that it is predicted too high in energy by the Koopmans-based method. In $\mathbf{5}^{\bullet+}$ the second allowed transition is dominated by B_1 excitation, but as no other single excitation mixes strongly with the former one, its prediction by the Koopmans-based method

TABLE 1: Comparison of the Observed and Calculated Spectra of the Polyene Radical Cations

	transition[a]	exp[b] $h\nu$/cm^{-1}	CASPT2[c] $h\nu$/cm^{-1} (f)[d] [deviation]	CASSCF assgn[f]	Koopmans-based $h\nu$/cm^{-1} [deviation]	Koopmans-based f[e] (assign)[f]
$\mathbf{1}^{\bullet+}$	$1^2B_g \rightarrow 1^2A_u$	18 500	19 900 (*0.014*) [+1400]	0.64 A_1 − 0.26 B_1	22 200 [+3700]	*0.086* (A_1)
	$1^2B_g \rightarrow 2^2A_u$	33 900	34 100 (*0.651*) [+200]	0.27 A_1 + 0.59 B_1	32 600 [−1300]	*0.150* (B_1)
$\mathbf{2}^{\bullet+}$	$1^2A_u \rightarrow 1^2B_g$	15 800	16 000 (*0.013*) [+200]	0.55 A_1 − 0.31 B_1	18 900 [+3100]	*0.166* (A_1)
	$1^2A_u \rightarrow 2^2B_g$	27 400	27 200 (1.001) [−200]	0.47 A_1 + 0.26 B_1	24 800 [−2600]	*0.223* (B_1)
$\mathbf{3}^{\bullet+}$	$1^2B_g \rightarrow {}^2A_u$	13 500	13 400 (*0.016*) [−100]	0.50 A_1 − 0.27 B_1	16 200 [+2700]	*0.241* (A_1)
	$1^2B_g \rightarrow 2^2A_u$	23 100	23 100 (*1.370*) [0]	0.24 A_1 + 0.47 B_1	20 100 [−3000]	*0.295* (B_1)

[a] Calculations were carried out in C_{2h} symmetry. [b] Reference 13. [c] Reference 36. [d] Oscillator strengths, calculated on the basis of CASSCF wavefunctions and CASPT2 energy differences. [e] Oscillator strengths, calculated as explained in the Introduction. [f] In terms of A and B type excitations, numbered from lower to higher energies.

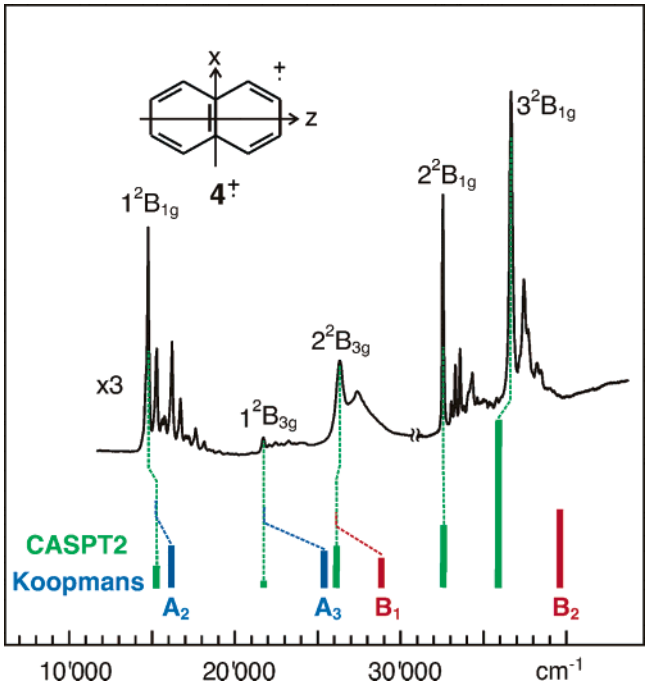

Figure 2. Ar matrix spectrum of $\mathbf{4}^{\bullet+}$ and predicted band positions and intensities from CASSCF/CASPT2 (green) and from Koopmans-based calculations (blue and red). For details see Table 2.

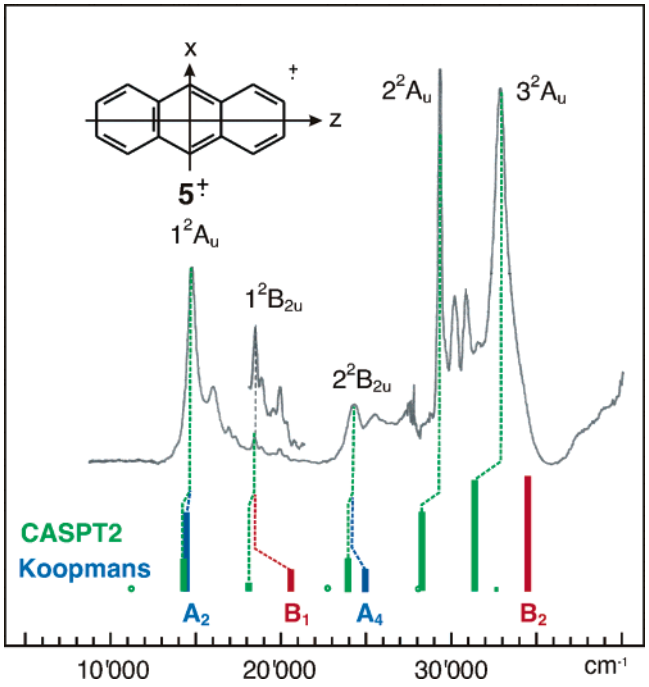

Figure 3. Ar matrix spectrum of $\mathbf{5}^{\bullet+}$ and predicted band positions and intensities from CASSCF/CASPT2 (green) and from Koopmans-based calculations (blue and red). For details see Table 2.

TABLE 2: Comparison of Observed and Calculated Spectra of the Radical Cations of Napthalene ($\mathbf{4}^{\bullet+}$) and Anthracene ($\mathbf{5}^{\bullet+}$)

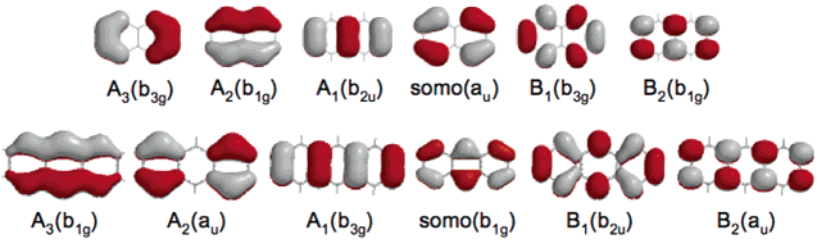

	transition[a]	exp[b] $h\nu$/cm^{-1}	CASPT2[c] $h\nu$/cm^{-1} (f)[d] [deviation]	CASSCF assgn[f]	Koopmans-based $h\nu$/cm^{-1} [deviation]	Koopmans-based f[e] (assign)[f]
$\mathbf{4}^{\bullet+}$	$1^2A_u \rightarrow 1^2B_{1g}$	14 840	15 240 (*0.042*) [+400]	0.69 A_2	16 130 [+1290]	*0.082* (A_2)
	$1^2A_u \rightarrow 1^2B_{3g}$	21 700	21 780 (*0.003*) [+80]	0.45 A_3 + 0.24 B_1	25 330 [+3630]	*0.071* (A_3)
	$1^2A_u \rightarrow 2^2B_{3g}$	26 210	26 310 (*0.081*) [−80]	0.40 B_1 + 0.13 A_3 + 0.11 C	28 790 [+2580]	*0.057* (B_1)
	$1^2A_u \rightarrow 2^2B_{1g}$	32 430	32 100 (*0.120*) [−330]	0.31 B_2 + 0.35 C	39 500 [+7070]	*0.153* (B_2)
	$1^2A_u \rightarrow 3^2B_{1g}$	36 700	35 810 (*0.390*) [−890]	0.45 C + 0.14 B_2		
$\mathbf{5}^{\bullet+}$	$1^2B_{1g} \rightarrow 1^2A_u$	14 440	14 290 (*0.061*) [−150]	0.62 A_2	14 330 [−110]	*0.151* (A_2)
	$1^2B_{1g} \rightarrow 1^2B_{2u}$	18 150	17 710 (*0.025*) [−440]	0.57 B_1	20 230 [+2080]	*0.044* (B_1)
	$1^2B_{1g} \rightarrow 2^2B_{2u}$	23 950	23 590 (*0.065*) [−360]	0.44 A_4 + 0.10 C	24 580 [+630]	*0.066* (A_4)
	$1^2B_{1g} \rightarrow 2^2A_u$	28 950	27 950 (*0.153*) [−1000]	0.37 C + 0.22 A_2	34 140 [+5190]	*0.223* (B_2)
	$1^2B_{1g} \rightarrow 3^2A_u$	32 420	30 990 (*0.212*) [−1430]	0.35 C + 0.18 A_2		

[a] Calculations were carried out in D_{2h} symmetry. [b] $\mathbf{4}^{\bullet+}$: ref 31, Figure 2. $\mathbf{5}^{\bullet+}$: Figure 3. [c] $\mathbf{4}^{\bullet+}$: ref 31. [d] Oscillator strengths, calculated on the basis of CASSCF wavefunctions and CASPT2 energy differences. [e] Oscillator strengths, calculated as explained in the Introduction. [f] In terms of A and B type excitations, numbered from lower to higher energies.

is slightly better that in the above case of $\mathbf{4}^{\bullet+}$. The third band in the spectrum of $\mathbf{4}^{\bullet+}$ is mainly due to the B_1 excitation, but the CASSCF calculations indicate again strong mixing with A_3 and with C-type excitations; hence the Koopmans-based prediction is again off by ca. 2500 cm^{-1}. In $\mathbf{5}^{\bullet+}$ the third allowed transition is a bit "purer" (A_4) and the absence of another dominant excitation indicates that the Koopmans-based prediction is quite close to experiment in this case.

The higher energy UV bands in the spectra of $\mathbf{4}^{\bullet+}$ and $\mathbf{5}^{\bullet+}$ cannot be modeled by the simple Koopmans method, which predicts the next transition to correspond to B_2 excitation in both cases, because CASSCF calculations indicate strong mixing with C-type excitations that are not amenable to a one-electron treatment.

In summation, the examples of $\mathbf{4}^{\bullet+}$ and $\mathbf{5}^{\bullet+}$ tell us that the Koopmans-based method works, even if the weight of the dominant configuration in the CASSCF wavefunction is lower than 50%, provided that the excited state is dominated by a single excited configuration, but that it predicts bands too high in energy if a second configuration makes a significant contribution. The assignments of the dominant excitations for the lower energy bands are the same, and CI can be confidently predicted when MOs of the same symmetry lie close in energy.

3. Biphenylene Radical Cation. For this work we have remeasured the optical spectrum of the biphenylene radicalcation (**6**$^{\bullet+}$), which had been previously observed in a *sec*-butyl ζ-chloride glass,[39] in an Ar matrix. Furthermore, we carried out CASSCF/CASPT2 calculations, the results of which are listed in Table 3, where the orbitals that are involved in the observed electronic transitions are shown. The Ar matrix spectrum and the calculations are graphically compared in Figure 4.

The weak first band contains resolved structure due to several vibrations, and its maximum can therefore not be determined unambiguously (we asssume that it is around 12 000 cm^{-1}). Its position is predicted well by both procedures, as is that of the second band (A_3) where two vibrational progressions are visible. The position of the B_2 band, which is partly masked by absoprtions of neutral **6**, is predicted correctly by CASPT2, but the calculated transition moment is incompatible with the observation that its intensity is similar to that of the A_3 band, which is indeed what the Koopmans-based method predicts (further investigation is needed to clarify this discrepancy). The B_2 band is too high by the Koopmans-based calculation, but this may again be due to CI with C-type excitations. The CASSCF calculations assign the intense UV transition to a transition that is dominated by a C-type excitation, which cannot be accounted for by the Koopmans method.

4. Larger Systems. We now move on to examine some radical cations that are too large for CASSCF-CASPT2 calculations with an adequate active space. To study most radical cations in solution, they must be protected by sterically demanding alkyl groups to confer some kinetic stability as well as thermodynamic stability onto them. Komatsu and co-workers have used bicyclo[2.2.2]octenyl "protecting groups" to study a wide range of otherwise unstable systems, several of which have even proven isolable.[40]

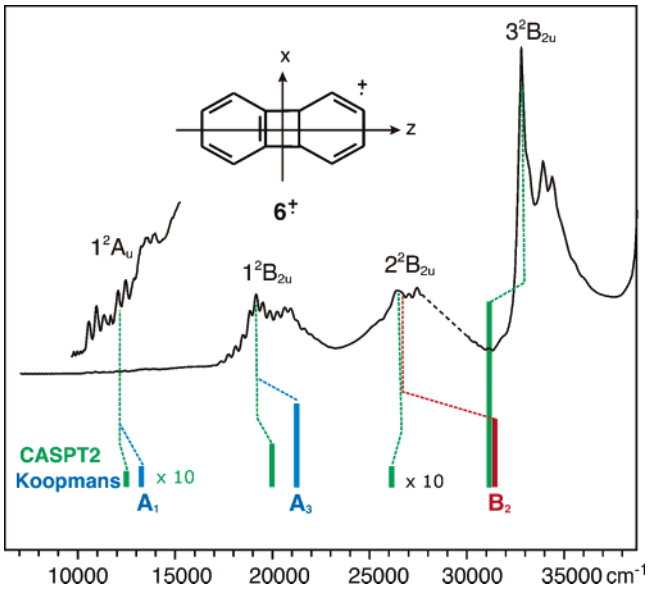

Figure 4. Ar matrix spectrum of **6**$^{\bullet+}$ and predicted band positions and intensities from CASSCF/CASPT2 calculations.

Figures 5 and 6 compare the observed and predicted spectra for the protected naphthalene and anthracene radical cation systems, **7**$^{\bullet+}$ and **8**$^{\bullet+}$,[41] and Table 4 compares the experimental data to the results of the Koopmans-type calculations and the orbitals involved in the excitations are shown in Table 5.

These solution spectra are of course less well resolved than the Ar matrix spectra shown in Figures 2 and 3, but the π systems are identical to those of **4**$^{\bullet+}$ and **5**$^{\bullet+}$ which are clearly expressed in analogies between the two spectra that greatly help in their assignment although the spectra are generally red-shifted as a consequence of the heavy alkyl substitution.

In the spectrum of **7**$^{\bullet+}$, the shoulder at ca. 21 100 cm^{-1} is probably due to the second transition ($1^2A_u \rightarrow 1^2B_{3g}$ in **4**$^{\bullet+}$) whereas the peak at ca. 29 100 cm^{-1} corresponds to the $1^2A_u \rightarrow 2^2B_{1g}$ transition in **4**$^{\bullet+}$. The intense peak at 31 900 cm^{-1} corresponds undoubteldy to the $1^2A_u \rightarrow 3^2B_{1g}$ transition in **4**$^{\bullet+}$, which cannot be predicted by the Koopmans-based method because the excited state is dominated by C-type excitations.

In the spectrum of **8**$^{\bullet+}$ the weak second B-type transition ($1^2B_{1g} \rightarrow 1^2B_{1u}$ in **5**$^{\bullet+}$) has shrunk to a series of wiggles between 15 000 and 20 000 cm^{-1} but by virtue of the general red shift the solution spectra reveal an additional intense UV transition that was not detected in the parent radical cation. However, we are in no position to assign this transition, which is probably also dominated by C-type excitations.

The equilibrium structure found for the radical cation of naphthalene derivative **7**$^{\bullet+}$ has effective D_2 symmetry because it is twisted by 19.0° about the central C−C bond of the naphthalene ring (the sum of the absolute values of the dihedral angles about one six-membered ring is 53.0°). This structure is 11.5 kcal/mol more stable than a D_{2h} structure where the naphthalene ring is constrained to be planar; hence the D_2 structure is used in the comparison of the calculated with the observed spectrum. The position of the first band of **7**$^{\bullet+}$ is predicted as accurately as for the unsubstituted compound, **4**$^{\bullet+}$, demonstrating that the effects of the octaalkyl substitution and of the significant twisting of the aromatic ring are handled well by the Koopmans-based calculations. According to our analysis, the weak second and the more intense third band correspond to A_5 and B_1 excitation, respectively. It seems likely that the mixing between these two configurations (which are already of the same

TABLE 3: Comparison of the Observed and Calculated Electronic Spectra of the Biphenylene Radical Cation (6$^{\bullet+}$)

transition[a]	exp[b] $h\nu$/cm^{-1}	CASPT2[c] $h\nu$/cm^{-1} (f)[d] [deviation]	CASSCF assgn[f]	Koopmans-based $h\nu$/cm^{-1} [deviation]	Koopmans-based f[e] (assign)[f]
$1^2B_{3g} \rightarrow 1^2A_u$	∼12 000	12 500 (*0.004*) [+500]	0.64 A_1	13 300 [+1300]	*0.005* (A_1)
$1^2B_{3g} \rightarrow 1^2B_{2u}$	19 230	20 000 (*0.104*) [+770]	0.63 A_3 + 0.08 C[f]	21 200 [+1970]	*0.201* (A_3)
$1^2B_{3g} \rightarrow 2^2B_{2u}$	26 530	26 100 (*0.005*) [−430]	0.42 B_2 + 0.16 C[a]	31 500 [+4970]	*0.168* (B_2)
$1^2B_{3g} \rightarrow 3^2B_{2u}$	32 790	31 300 (*0.444*) [−1490]	0.38 C[a] + 0.07 A_3		

[a] Calculations were carried out in D_{2h} symmetry. [b] Figure 4. [c] This work. [d] Oscillator strengths, calculated on the basis of CASSCF wavefunctions and CASPT2 energy differences. [e] Oscillator strengths, calculated as explained in the Introduction. [f] In terms of A and B type excitations, numbered from lower to higher energies.

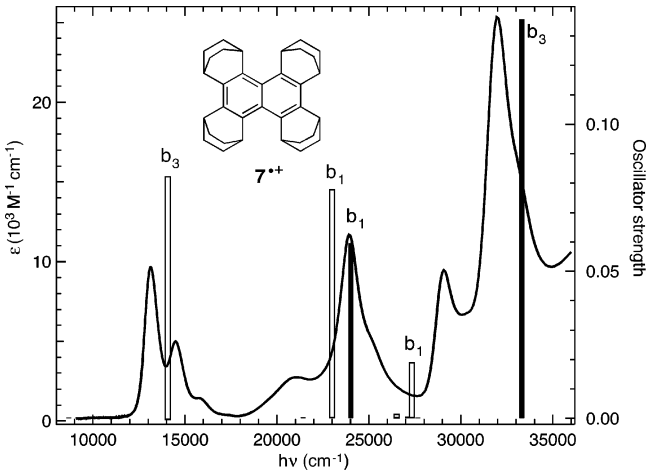

Figure 5. Observed and Koopmans-based calculation of the optical spectra of protected naphthalene radical cation **7**•+. Type A transitions are indicated by open bars; type B transitions, by full bars.

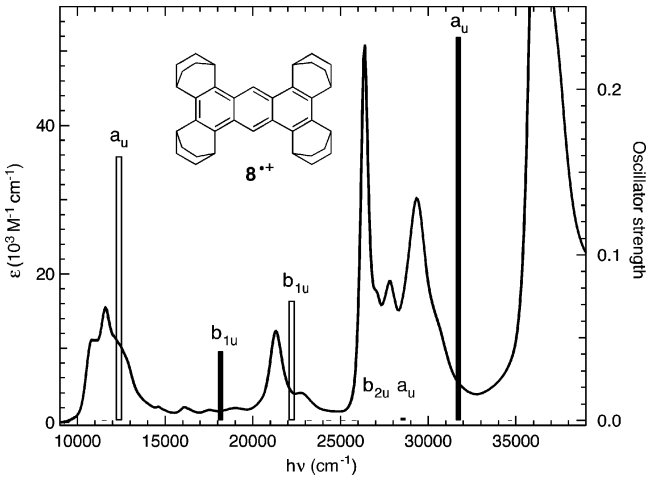

Figure 6. As for Figure 5, for the protected anthracene radical cation **8**•+. Type A transitions are indicated by open bars; type B transitions, by full bars.

TABLE 4: Comparison of Koopmans-Based Calculations and Experiment for Protected Naphthalene and Anthracene Radical Cations (7•+ and 8•+)

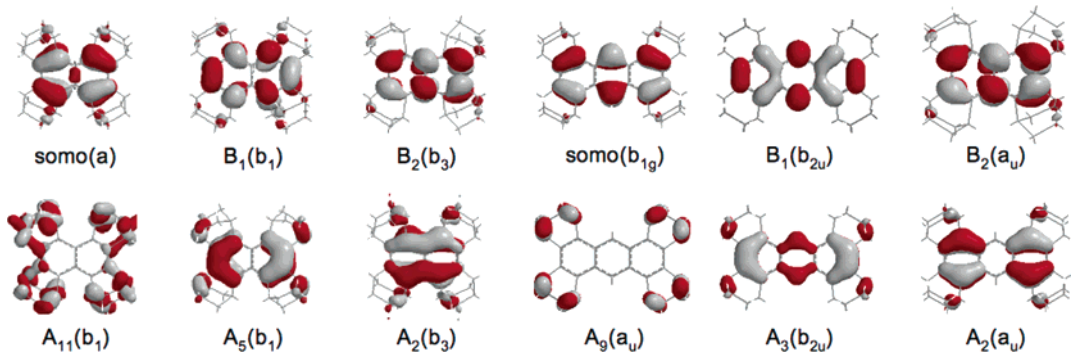

compd (symm)	obs *hν* (*ϵ*)	calculated (Koopmans-based) *hν* (*f*) [deviation]	assgn (symm)
7•+ (D_2)	13 100 (9700)	14 120 (*0.083*) [+1020]	A_2 (b_3)
	21 100 (2700)	22 990 (*0.078*) [+1890]	A_5 (b_1)
	23 900 (11 700)	24 020 (*0.060*) [+120]	B_1 (b_1)
	29 100 (9500)	27 320 (*0.019*) [−1780]	A_{11} (b_1)
	31 900 (25 300)	33 310 (*0.136*) [+1410]	B_2 (b_3)
8•+ (D_{2h})	11 600 (15 500)	12 340 (*0.159*) [+1540]	A_2 (a_u)
	16 100 (2090)	18 160 (*0.041*) [+2060?]	B_1 (b_{2u})
	21 300 (12 300)	22 210 (*0.072*) [+910]	A_3 (b_{2u})
	26 400 (50 800)	28 570 (*0.0016*) [+2170]	A_9 (a_u)
	29 300 (30 200)	31 700 (*0.234*) [+2400]	B_2 (a_u)
	36 200 (92 800)		

symmetry in D_{2h}) and with higher lying states is responsible for the poor agreement with the experimental pattern of bands, especially their intensities.

The Koopmans calculations assign the sharp third band to electron promotion from a σ(CH−CH$_2$) MO to the SOMO. It is, however, probable that this relatively high-lying excitation mixes with other ones, an effect that these calculations cannot account for. The b_3 orbital B_2 is at about the right energy to account for the 31 900 cm^{-1} band in **7**•+, but assignments become less certain as the excitation energies increase and type C transitions gain importance.

The protected anthracene, **8**•+, is far less strained and therefore has a D_{2h} equilibrium structure. Its first band is predicted even more accurately than that in the protected naphthalene, **8**•+. The next two transitions are also predicted quite well by the Koopmans-type calculations although the intensity of the B_1 transition is predicted too high (as it was already in the parent compound, **5**•+). As mentioned above, the intense bands above 25 000 cm^{-1}, which in **5**•+ involve strong contributions from C-type excitations, cannot be assigned properly by Koopmans' procedure, which ignores these excitations. Certainly, excitation from the A_9 MO will contribute prominently to one or both of these transitions.

The protected biphenylene[41] (**9**•+) has far fewer nonbonded interactions than the protected napththalene and therefore maintains D_{2h} symmetry. Its spectrum is shown in Figure 7, and the data are summarized in Table 5, in which the orbitalsinvolved in the allowed transitions are shown. As in the parent compound, **6**•+, the A_1 transition is predicted to have a very low intensity and it is in fact too weak to be observed in the spectrum of **9**•+. As in **6**•+, the next two bands are of similar intensities (cf. Figure 4), but in **9**•+ the first one is red- and the second one is blue-shifted by ca. 2500 cm^{-1}. Nevertheless, the

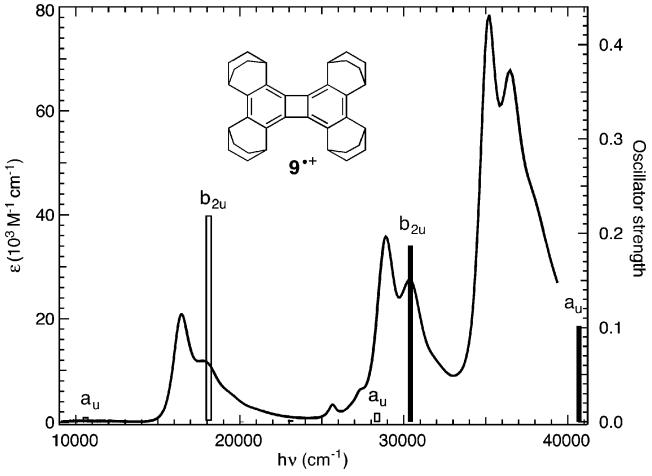

Figure 7. Observed and Koopmans-based calculation of the optical spectra of protected biphenylene radical cation $\mathbf{9}^{\bullet+}$. Type A transitions are indicated by open bars; type B, by full bars.

TABLE 5: Comparison of Koopmans-Based Calculations and Experiment for $\mathbf{9}^{\bullet+}$, D_{2h} Symmetry

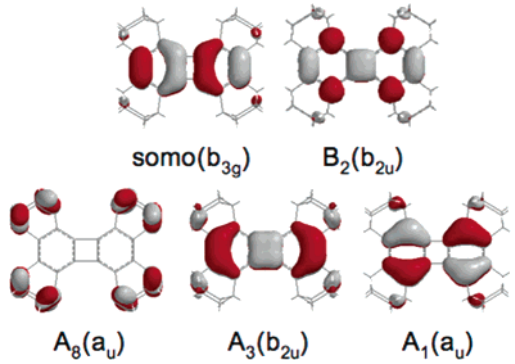

obs	calculated (Koopmans-based)	
$h\nu$ (ϵ)	$h\nu$ (f) [deviation]	assgn (symm)
	10 570 (*0.004*) [unobs]	A_1 (a_u)
16 450 (20 300)	18 150 (*0.219*) [+1700]	A_3 (b_{2u})
28 900 (35 800)	28 350 (*0.009*) [−]	A_8 (a_u,σ_π)
	30 400 (*0.187*) [+1500]	B_2 (b_{2u})
35 200 (78 500)		

assignment of these bands is the same as in the parent radical cation (A_3 and B_1, respectively).

There is a small sharp band at 25 600 cm^{-1} (ϵ 3500) that might conceivably correspond to one of several weak predicted transitions involving promotions from σ-MOs, such as, for example, A_4 (b_{1u}), predicted at 23 000 cm^{-1}, or A_8, which is a $CHCH_2$ σ bond orbital. As C-type transitions are mainly responsible for the intense UV band, we do not believe that Koopmans-based calculations are likely to give good descriptions of the higher energy transitions.

The radical cations of the protected cyclooctatetraene derivatives, $\mathbf{10}^{\bullet+}$ [42] and $\mathbf{11}^{\bullet+}$,[43] are a particularly interesting pair: in the bicyclo[2.2.2]octenyl-protected compound $\mathbf{10}^{\bullet+}$ the double bonds are internal to the bicyclooctene rings, which are thus connected by substantially twisted single bonds to evade steric repulsion. In contrast, the bicyclo[2.1.1]hexenyl groups in $\mathbf{11}^{\bullet+}$ undergo much less repulsion, whereas introducing double bonds into these groups would result in substantial angular strain. As a consequence, the double bonds are arranged exocyclic to the bicyclic groups, which causes the cyclooctatetraene ring to be

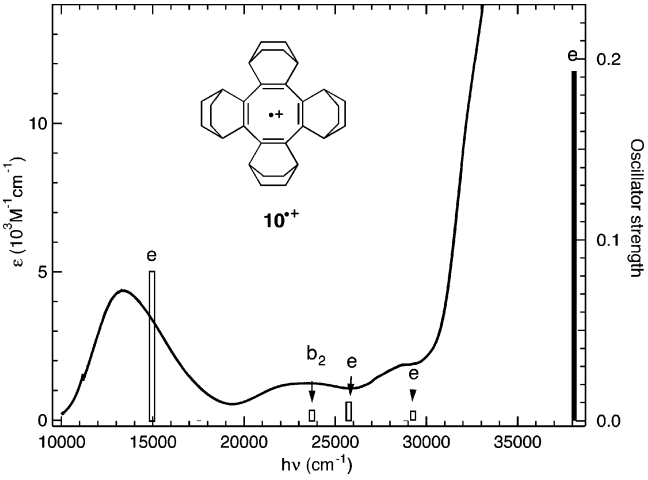

Figure 8. Optical spectrum of $\mathbf{10}^{\bullet+}$ and results from Koopmans-based calculations. Type A transitions are indicated by open bars; type B, by full bars.

TABLE 6: Comparison of Koopmans-Based Calculations and Experiment for $\mathbf{10}^{\bullet+}$, Calculated in D_{2d} Symmetry

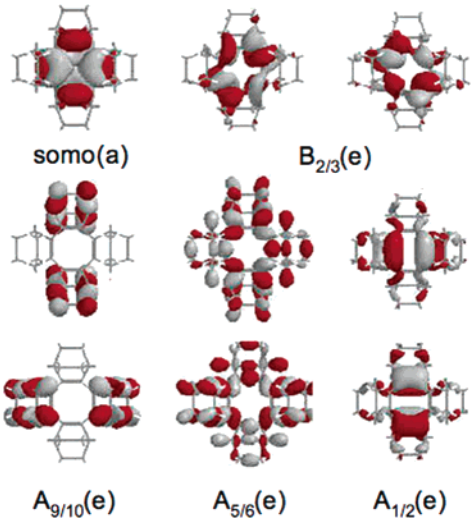

obs	Koopmans-based	
$h\nu$ (ϵ)	$h\nu$ (f) [deviation]	assgn (symm)
13 400 (4360)	14 940 (*0.082*) [+1540]	A_{1-2} (e)
23 500 (1240)	23 700 (*0.006*) [+200]	A_3 (b_2)
	25 730 (*0.010*) [+2230]	A_{5-6} (e)
28 900 (1870)	29 250 (*0.005*) [+350]	$A_{9,10}$ (e)
	30 060 (*0*)	A_{11} (a_1)
~32 000 sharp rise	{38 080 (*0.193*)}	{B_{2-3} (e)}

most stable when it is planar. Thus the spectra of the two radical cations are quite dissimilar.

For the calculation of excited states we used a structure optimized within D_{2d} symmetry for $\mathbf{10}^{\bullet+}$.[44] In this structure the dihedral angles θ between the C=C bonds are 54.4°, so the C_8 ring in $\mathbf{10}^{\bullet+}$ is almost as strongly puckered as it is in neutral cyclooctatetraene (θ = 57.9°)[45] and much more so than in the unsubstituted cyclooctatetraene radical cation ($\theta_{UMP2/6-31G^*}$ = 42.3°).[28] The optical spectrum of $\mathbf{10}^{\bullet+}$ is compared with the results from Koopmans-based calculations in Figure 8, and the data are summarized in Table 6, in which the orbitals involved in the transitions are shown.

Due to the puckering of the C_8 ring significant σ,π mixing occurs, and the weak transitions from both $A_{9-10} \rightarrow$ SOMO and $A_{5-6} \rightarrow$ SOMO, which appear to be observed in the spectrum, arise from σ_{CC},σ_{CH} combination orbitals with little π(C=C)

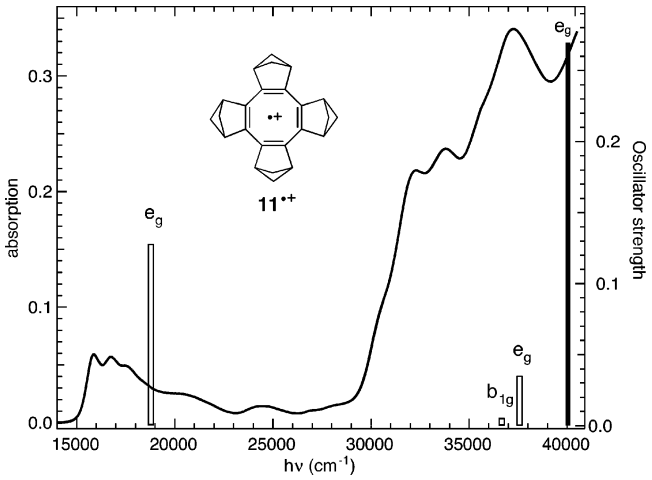

Figure 9. Observed and Koopmans-based calculation of the optical spectrum of **11**$^{\bullet+}$. Type A transitions are indicated by open bars; type B, by full bars.

TABLE 7: Comparison of Koopmans-Based Calculations and Experiment for 11$^{\bullet+}$ Calculated in D_{4h} Symmetry

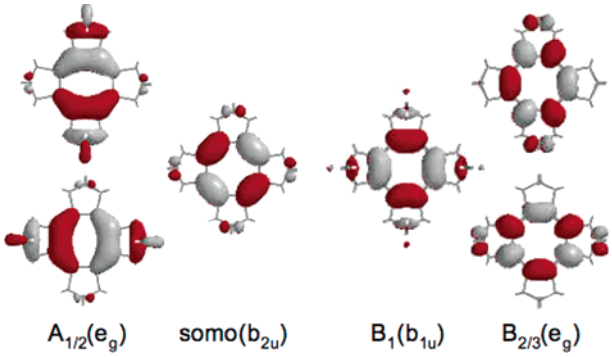

obs	Koopmans-based	
hν (*abs*)	*hν* (*f*) [deviation]	assgn (symm)
15 800 (*0.059*)	18 820 (*0.128*) [+3040]	A_{1-2} (e_g)
~19 000 sh (*0.025*)		
24 400 (*0.014*)		
32 300 (*0.218*)	36 630 (*0.005*)	A_9 (b_{1g})
33 800 (*0.237*)	37 810 (*0.035*) [+4010?]	A_{10-11} (e_g)
37 300 (*0.341*)	40 040 (*0.269*) [+2740?]	B_{2-3} (e_g)

character. In contrast, the first, intense band is due to excitations within π-MOs centered largely in the C_8 ring

In contrast, the bicyclohexene protected cyclooctatetraene radical cation **11**$^{\bullet+}$ shows the spectrum shown in Figure 9, which also contains the Koopmans-based predictions (data in Table 7, with the orbitals involved in the allowed transitions shown) using the D_{4h} structure of this compound. As **11**$^{\bullet+}$ is rather unstable, it was impossible to determine ϵ with any accuracy.

A single allowed low-energy transition leading to a degenerate excited state is predicted (in addition to the dipole forbidden B_1 (b_{1u}) transition which is predicted at 12 000 cm^{-1}); i.e. the structure of the first band should be vibronic. No other high-intensity bands are predicted up to 40 000 cm^{-1}. However, a strong configuration interaction is expected to prevail between the three e_g states, and this may be the reason for the rather large differences between the Koopmans-based transition energies and the observed bands in **11**$^{\bullet+}$.

Recently, Rathore and Burns published the optical spectrum of the isolable radical cation of hexa-*peri*-*tert*-butylhexabenzo-

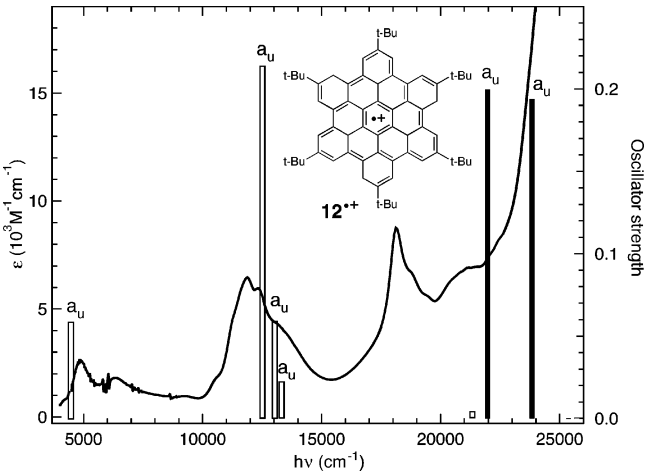

Figure 10. Electronic absorption spectrum **12**$^{\bullet+}$and results of Koopmans-based calculations for the hexamethyl derivative. Type A transitions are indicated by open bars; type B, by full bars.

TABLE 8: Comparison of Koopmans-Based Calculations and Experiment for 12$^{\bullet+}$, Calculated in C_{2h} Symmetry

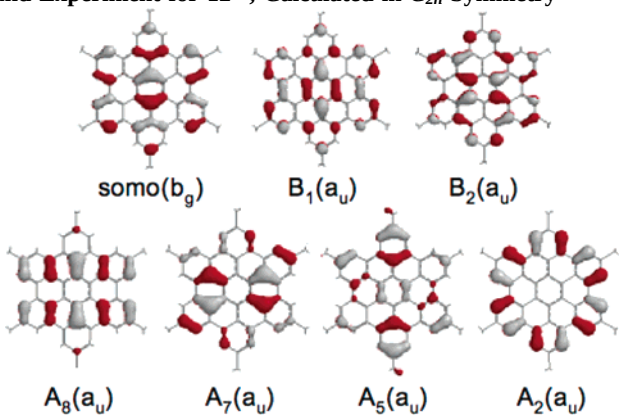

obs	Koopmans-based	
	allowed	
hν (*ε*)	*hν* (*f*) [deviation]	assgn (symm)
4 900 (2600)	4 460 (*0.058*) [−440]	A_2 (a_u)
~10 600 sh (1860)	12 500 (*0.214*) [~+1900]	A_5 (a_u)
11 900 (6320)	13 030 (*0.059*) [~+1130]	A_7 (a_u)
~13 400 sh (4320)	13 320 (*0.022*)	A_8 (a_u)
18 150 (8760)	21 250 (*0.0031*) [~+3100]	A_9 (a_u)
	21 390 (*0.0032*)	A_{10} (a_u)
~21 150 sh (6440)	21 970 (*0.200*)	B_1 (a_u)
	23 840 (*0.194*)	B_2 (a_u)
~25 000 sharp rise		

coronene, **12**$^{\bullet+}$,[46] which has a 42-atom π system consisting of a symmetrical cluster of 13 fused aromatic rings. As we do not expect that changing the alkyl groups will significantly affect the calculated spectrum, we carried out the calculations on the hexamethyl compound. The symmetry obtained was C_{2h} (the radical cation calculation started from a C_{6h} neutral structure, the optimization lowered the symmetry to C_{2h}). When no symmetry constraints were imposed, the energy decreased by 0.67 kcal/mol and the benzenoid frame of **12**$^{\bullet+}$ assumed a slightly undulating structure (presumably due to vibronic coupling of the ground state with low-lying excited states). However, we elected to carry out the NCG and DCG calculations for the planar species, so that transitions of **12**$^{\bullet+}$ that might otherwise have very small transition moments are electric dipole forbidden. The calculated transitions are compared with the spectrum in Figure 10 and Table 8, where the orbitals involved are shown.

$12^{\bullet+}$ has seven π-orbitals, and hence seven excited configurations, of a_u symmetry within a range of 14 000 cm^{-1} and all these configurations are expected to mix to form excited states. Nevertheless, an assignment of the low-energy part of the spectrum of $12^{\bullet+}$ appears to be possible on the basis of NCG calculations. According to these calculations $12^{\bullet+}$ should show an NIR band of appreciable intensity, due to the A_2 excitation, which was not detected in the original experiments.[46] As a consequence of this prediction, the experiment was repeated and the measurement was extended to 4000 cm^{-1}, whereupon this band was indeed found (see Figure 10), thus demonstrating the predictive power of Koopmans-based calculations.

The next band of $12^{\bullet+}$, which peaks at 11 900 cm^{-1}, presumably involves contributions from the A_5, A_7, and A_8 transitions that are predicted around 13 000 cm^{-1}. Within our model, we are tempted to assign the band at 18 150 cm^{-1} to the lowest energy component of the close-lying low-intensity A_9 and A_{10} transitions. However, the time-dependent density functional theory (TD-DFT) calculations listed in the Supporting Information indicate that a transition dominated by a C-type excitation is responsible for this band (which is predicted quite accurately by TD-DFT), which can therefore not be reproduced by Koopmans-type calculations. The two lowest energy type B bands (shown in red) are also a_u and may be responsible for the strong rise at 24 000 cm^{-1}. As usual, the overlapping bands leading to the sharp rise are not predicted by Koopmans-based methods and presumably involve more complex transitions.

In the Supporting Information we compare the results from Koopmans-based calculations with those from the popular TD-DFT method.[47−49] Hirata and co-workers have recently made an extensive comparison of electronic absorption spectra for aromatic hydrocarbon radical cations with TD-DFT calculations (carried out at the neutral compound geometry).[50] Surprisingly, although TD-DFT calculations include the effects of mixing singly excited configurations, and they are often found to give an analysis of the transitions that resembles that obtained from CASSCF/CASPT2 calculations (in cases where the comparison can be made), the calculated transition energies obtained for the first few bands are in most cases further from the experimental ones than those estimated by the Koopmans-based method that ignores the effects of configurational mixing. For the 12 compounds examined here (including the dihydroacenaphthalene and pyracene radical cations, presented only in the Supporting Information) the Koopmans-based calculations predict the energy of the first allowed transition closer to experiment than the TD-DFT calculations in 11 cases. The exceptions are 3^+, where both predictions are off by over 2200 cm^{-1} and 12^+, where both are within 500 cm^{-1} of the observed value.

TD-DFT calculations take over an order of magnitude longer than the two single point calculations that are necessary to obtain the intensities for the Koopmans-based method for most of these compounds, and even longer for the larger ones.

Conclusion

The results reported here show that it is possible to rationalize and predict both A-type (doubly occupied MO to SOMO) and B-type (SOMO to virtual MO) electronic transitions in the optical spectra of radical cations in terms of simple *orbital energy differences* calculated for the closed shell neutral (NCG, for A-type transitions) or the dication (DCG, for B-type transitions) at the geometry of the radical cation under investigation. In the former case, one makes use of the approximations inherent in Koopmans' theorem, whereas in the latter case, where energy differences between *virtual* MOs are used, no comparable theoretical framework exists to justify this method. However, it appears that the fortuitous cancellation of the energetic consequences of (a) relaxing the wavefunction and (b) decreasing the correlation energy on going from the neutral to the radical cation (which forms the basis of the numerical success of Koopmans' theorem) applies similarly in the DCG calculations.

Of course the above-described methods cannot account for the effects of mixing between different excited electronic configurations. However, the considerable success of calculations based on Koopmans' theorem for the assignment of photoelectron spectra[51] shows that these effects may be absorbed into a one-electron picture if they are not predominant.

Often the first one to two absorption bands of radical cations correspond to transitions involving states that can be modeled reasonably well by single electronic configurations. The energies of such transitions can be predicted quite reliably (i.e., within a few hundred wavenumbers) by the above Koopmans'-type methods, in fact, often more reliably than by the currently popular TD-DFT methods requiring calculations that can take orders of magnitude longer to complete. Strong deviations between the Koopmans-based predictions and experiment for the first few absoprtion bands of radical cations are usually indicative of extensive configurational mixing, even in this region, such as it prevails, e.g., in polyene radical cations.

The simple approach presented in this paper fails whem C-type transitions, i.e., excitations from doubly occupied to virtual MOs, come into play, as it is often the case with UV-absorption bands of radical cations. First, the energies of C-type excited configurations cannot be associated with orbital energy differences, and second, many-electron calculations show that such configurations often undergo extensive mixing among themselves and sometimes with A- or B-type excited configurations. Thus, the Koopmans-based methods can and should not be used to assign higher lying excited states of radical cations.

Using Weinhold's NBO program, we also calculated transition moments for excitations between states described by single configurations. Often the general pattern of bands that emerge from those calculations match quite well with the experimental ones, which indicates that a simple one-electron picture of electronic excitations in radical cations may be quite valid. Again, pronounced incompatibilities between experiment and calculations indicate interference by C-type excitations and/or configurational mixing.

Acknowledgment. This paper is dedicated to the memory of Edgar Heilbronner who passed away on August 25, 2006, and who had pioneered the application of Koopmans' theorem to the interpretation of photoelectron spectra. This work is part of project 200020-113268 of the Swiss National Science Foundation. S.F.N. thanks the U.S. National Science Foundation for partial support of this work under grant CHE-0240197. D.Y. thanks the Japan Society for the Promotion of Science for a Research Fellowship for Young Scientists (No. 16-1199). R.R. thanks the National Science Foundation for a career award.

Supporting Information Available: Cartesian coordinates and energies of all optimized structures, including those of the naphthalene derivatives that are not shown in the paper. Results of TD-DFT calculations of $1^{\bullet+}$−$12^{\bullet+}$ as well as dihydroacenaphthalene and pyracene radical cations. This material is available free of charge via the Internet at http://pubs.acs.org.

References and Notes

(1) Haselbach, E.; Schmelzer, A. *Helv. Chim. Acta* **1971**, *54*, 1575−80.

(2) Haselbach, E.; Schmelzer, A. *Helv. Chim. Acta* **1972**, *55*, 1745−52.

(3) Haselbach, E.; Lanyiova, Z.; Rossi, M. *Helv. Chim. Acta* **1973**, *56*, 2889−99.

(4) Haselbach, E.; Bally, T.; Gschwind, R.; Klemm, U.; Lanyiova, Z. *Chimia* **1979**, *33*. 405−411.

(5) Zahradník, R.; Čársky, P.; Slanina, Z. *Collect. Czech. Chem. Commun.* **1973**, *38*, 1886−98.

(6) Shida, T.; Nosaka, Y.; Kato, T. *J. Phys. Chem.* **1978**, *82*, 695−698.

(7) Shida, T.; Haselbach, E.; Bally, T. *Acc. Chem. Res.* **1984**, *17*, 180−6.

(8) Buschow, K. H. J.; Dieleman, J.; Hoijtink, G. J. *Mol. Phys.* **1964**, *7*, 1−9.

(9) Čársky, P.; Zahradník, R. *Top. Curr. Chem.* **1973**, *43*, 1−55.

(10) Koopmans, T. *Physica* **1933**, *1*, 104−113.

(11) Haselbach, E.; Klemm, U.; Buser, V.; Gschwind, R.; Jungen, H.; Kloster-Jensen, E.; Maier, J. P.; Marthaler, O.; Christen, H.; Baertschi, P. *Helv. Chim. Acta* **1981**, *64*, 823−34.

(12) Haselbach, E.; Klemm, U.; Gschwind, R.; Bally, T.; Chassot, L.; Nitsche, S. *Helv. Chim. Acta* **1982**, *65*, 2464−71.

(13) Bally, T.; Nitsche, S.; Roth, K.; Haselbach, E. *J. Am. Chem. Soc.* **1984**, *106*, 3927−33.

(14) Nelsen, S. F.; Cunkle, G. T.; Evans, D. H.; Clark, T. *J. Am. Chem. Soc.* **1983**, *105*, 5928−5929.

(15) Nelsen, S. F.; Blackstock, S. C.; Yumibe, N. P.; Frigo, T. B.; Carpenter, J. E.; Weinhold, F. *J. Am. Chem. Soc.* **1985**, *107*, 143−149.

(16) Nelsen, S. F.; Frigo, T. B.; Kim, Y.; Blackstock, S. B. *J. Am. Chem. Soc.* **1989**, *111*, 5387−5397.

(17) Nelsen, S. F.; Tran, H. Q.; Ismagilov, R. F.; Chen, L.-J.; Powell, D. R. *J. Org. Chem.* **1998**, *63*, 2536−2543.

(18) Clark, T.; Teasley, M. F.; Nelsen, S. F.; Wynberg, H. *J. Am. Chem. Soc.* **1987**, *109*, 5719−5724.

(19) Rauhut, G.; Chandrasekhar, J.; Alex, A.; Steinke, T.; Clark, T. *VAMP 5.0*; Oxford Molecular: Oxford, U.K., 1994.

(20) Bally, T. In *Radical Ionic Systems*; Lund, A., Shiotani, M., Eds.; Kluwer: Dortrecht, 1991; pp 3−54.

(21) Jordan, K. D.; Burrow, P. D. *Chem. Rev.* **1987**, *87*, 557−588.

(22) Chen, D.; Gallup, G. A. *J. Chem. Phys.* **1990**, *93*, 8893−8901.

(23) Nelsen, Stephen F.; Konradsson, A. E.; Telo, J. P. *J. Am. Chem. Soc* ***2005****, 127*, 920−925.

(24) Nelsen, S. F.; Weaver, M. N.; Telo, J. P.; Zink, J. I. *J. Am. Chem. Soc* **2005**, *127*, 11611−11622.

(25) Nelsen, S. F.; Weaver, M. N.; Telo, J. P.; Lucht, B. L.; Barlow, S. *J. Org. Chem.* **2005**, *70*, 9326−9333.

(26) Bally, T.; Borden, W. T. *Rev. Comput. Chem.* **1999**, *13*, 1−97.

(27) Heilbronner, E.; Maier, J. P. In *Electron Spectroscopy: Theory, Techniques and Applications*; Brundle, C. R., Baker, A. D., Eds.; Academic Press: London, 1977; Vol. 1, pp 205−292.

(28) Bally, T.; Truttmann, L.; Dai, S.; Williams, F. *J. Am. Chem. Soc.* **1995**, *117*, 7916−7922.

(29) Truttmann, L.; Asmis, K. R.; Bally, T. *J. Phys. Chem.* **1995.**, *99*, 17844−17851.

(30) Zhu, Z.; Bally, T.; Wirz, J.; Fülscher, M. *J. Chem. Soc., Perkin Trans.* **1998**, *2*, 1083−1091.

(31) Bally, T.; Carra, C.; Fülscher, M.; Zhu, Z. *J. Chem. Soc., Perkin Trans.* **1998**, *2*, 1759−1765.

(32) Marcinek, A.; Adamus, J.; Huben, K.; Gebicki, J.; Bartczak, T. J.; Bednarek, P.; Bally, T. *J. Am. Chem. Soc.* **2000**, *122*, 437−443.

(33) Bally, T.; Zhu, Z.; Wirz, J.; Fülscher, M.; Hasegawa, J.-Y. *J. Chem. Soc., Perkin Trans.* **2000**, *2* 2311−2318.

(34) Bednarek, P.; Zhu, Z.; Bally, T.; Filipiak, T.; Marcinek, A.; Gebcki, J. *J. Am. Chem. Soc.* **2001**, *123*, 2377−2387.

(35) Müller, B.; Bally, T.; Gerson, F.; de Meijere, A.; von Seebach, M. *J. Am. Chem. Soc.* **2003**, *125*, 13776−13783.

(36) NBO 5.0. E. D. Glendening, J. K. Badenhoop, A. E. Reed, J. E. Carpenter, J. A. Bohmann, C. M. Morales, and F. Weinhold (Theoretical Chemistry Institute, University of Wisconsin, Madison, WI, 2001).

(37) Fülscher, M. P.; Matzinger, S.; Bally, T. *Chem. Phys. Lett.* **1995**, *236*, 167−176.

(38) Bally, T.; Roth, K.; Tang, W.; Schrock, R. R.; Knoll, K.; Park, L. Y. *J. Am. Chem. Soc.* **1992**, *114*, 2440−2446.

(39) Shida, T. *Electronic Absorption Spectra of Radical Ions*; Elsevier: Amsterdam, 1988.

(40) For a review, see: Komatsu, K.; Nishinaga, T. *Synlett* **2005**, 187−202.

(41) Matsuura, A.; Nishinaga, T.; Komatsu, K. *J. Am. Chem. Soc.* **2000**, *122*, 10007−10016. The spectrum reported as that of the protected benzene radical cation in this paper is under reinvestigation.

(42) Nishinaga, T.; Komatsu, K.; Sugita, N.; Lindner, H. J.; Richter, J. *J. Am. Chem. Soc.* **1993**, *115*, 11642−11643.

(43) Nishinaga, T.; Uto, T.; Komatsu, K. *Org. Lett.* **2004**, *6*, 4611−4613.

(44) (a) A C_1 structure 0.1 kcal/mol lower in energy was obtained when symmetry was not imposed, but it only had splittings of 0.3, 0.3, and 16.9 cm^{-1} for the $A_{1,2}$, $A_{4,5}$, and $A_{9,10}$ e symmetry orbitals at D_{2d} symmetry, so the spectrum is not significantly affected. Nevertheless, twisting in the bicyclooctene radical cation is easy, and the parent has a twist of 14° about its double bond.[43b] (b) Nelsen, S. F.; Reinhardt, L. A.; Tran, H. Q.; Clark, T.; Chen, G.-F.; Pappas, P. S.; Williams, F. *Chem. Eur. J.* **2002**, *8*, 1074−1081.

(45) Traetteberg, M. *Acta Chim. Scand.* **1966**, *20*, 1724−1726.

(46) Rathore, R.; Burns, C. L. *J. Org. Chem.* **2003**, *68*, 4071−4074.

(47) Burke, K.; Gross, E. K. U. In *Density Functionals: Theory and Applications*; Joubert, D., Ed.; Springer: Berlin, 1998; pp 116−146.

(48) Casida, M. E.; Jamorski, C.; Casida, K. C.; Salhub, D. R. *J. Chem. Phys.* **1998**, *108*, 4439−4449.

(49) Stratmann, R. E.; Scuseria, G. E.; Frisch, M. J. *J. Chem. Phys.* **1998**, *109*, 8218−8224.

(50) Hirata, S.; Head-Gordon, M.; Szczepanski, J.; Vala, M. *J. Phys. Chem. A* **2003**, *107*, 4940−4951.

(51) See, e.g.: Bock, H.; Ramsey, B. G. *Angew. Chem.* **1973**, *85*, 773. Bally, T.; Heilbronner, E. In *The Chemistry of Dienes and Polyenes*; Rappoport, Z., Ed.; John Wiley & Sons: New York, 1997.